# Effects of Charge Separation, Effective Concentration, and Aggregate Formation on the Phase Transfer Catalyzed Alkylation of Phenol

Scott E. Denmark,* Robert C. Weintraub, and Nathan D. Gould

Roger Adams Laboratory, Department of Chemistry, University of Illinois, Urbana, Illinois 61801, United States

S Supporting Information

ABSTRACT: The factors that influence the rate of alkylation of phenol under phase transfer catalysis (PTC) have been investigated in detail. Six linear, symmetrical tetraalkylammonium cations, Me_4N^+, Et_4N^+, $(n\text{-}Pr)_4N^+$, $(n\text{-}Bu)_4N^+$, $(n\text{-}Hex)_4N^+$, and $(n\text{-}Oct)_4N^+$, were examined to compare the effects of cationic radius and lipophilicity on the rate of alkylation. Tetraalkylammonium phenoxide·phenol salts were prepared, and their intrinsic reactivity was determined from initial alkylation rates with n-butyl bromide in homogeneous solution. The catalytic activity of the same tetraalkylammonium phenoxides was determined under PTC conditions (under an extraction mechanism) employing quaternary ammonium bromide catalysts. In homogeneous solution the range in reactivity was small (6.8-fold) for Me_4N^+ to $(n\text{-}Oct)_4N^+$. In contrast, under PTC conditions a larger range in reactivity was observed (663-fold). The effective concentration of the tetraalkylammonium phenoxides in the organic phase was identified as the primary factor influencing catalyst activity. Additionally, titration of active phenoxide in the organic phase confirmed the presence of both phenol and potassium phenoxide aggregates with $(n\text{-}Bu)_4N^+$, $(n\text{-}Hex)_4N^+$, and $(n\text{-}Oct)_4N^+$, each with a unique aggregate stoichiometry. The aggregate stoichiometry did not affect the PTC initial alkylation rates.
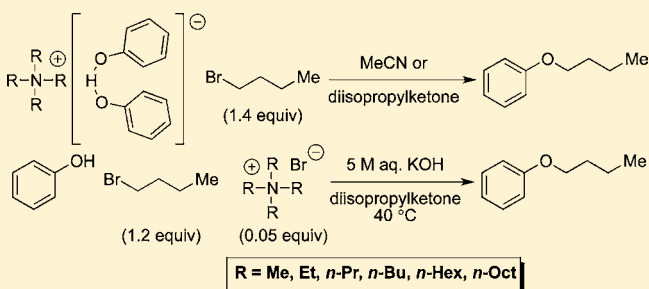
INTRODUCTION

Phase transfer catalysis (PTC) embodies the ideals of organic synthesis by providing a simple, cheap, and general protocol for a myriad of reactions.[1] Of the numerous types of reactions that are amenable to PTC, the most synthetically useful are those that make C−N, C−O, and C−C bonds.[2] Specifically, aliphatic nucleophilic substitution reactions employing nitrogen, oxygen, or carbon nucleophiles in combination with carbon electrophiles constitute the majority of the most synthetically useful PTC reactions. The preparative advantages of PTC for such alkylation reactions derive from its operational simplicity, ease of removal of byproducts, and enhanced reaction rates. In addition, PTC facilitates the use of inexpensive hydroxide bases and obviates the need for dipolar aprotic solvents. In fact, under PTC conditions, comparable rates are observed with little or no solvent in combination with the addition of a small amount (1−5 mol %) of a quaternary ammonium ion phase transfer catalyst.[3]

The preparative advantages of PTC are accompanied by mechanistic ambiguity that arises from the transport component and non-covalent ion pairing that make PTC a difficult system to study. The catalytic cycle of PTC necessarily involves at least one physical phenomenon (or step), distinguishing it from homogeneous catalysis wherein the entire catalytic cycle is comprised of chemical steps. Consequently, the selection of the optimum catalyst for a particular application remains a time-consuming, largely empirical exercise. The relative contributions of transport,

nucleophile activation, and nucleophile desolvation to catalytic activity have remained an outstanding question for nearly three decades. Accordingly, the *a priori* prediction of catalyst efficiency for any specific reaction remains an elusive objective.

Recently, we initiated a research program aimed at elucidating the structural features that govern the activity and enantioselectivity of quaternary ammonium ion phase transfer catalysts.[4] After evaluation of many quantitative structure–activity relationship (QSAR) models for catalyst activity in an enolate alkylation, we were led to the conclusion that the activity of quaternary ammonium ion catalysts could be well described with a combination of nonlinear equations with only a few molecular parameters. Nevertheless, we encountered a number of questions that could not be directly addressed in a quantitative manner with the initial data set. For example, throughout the study we had little to no indication that the actual *reactivity* of the quaternary ammonium·substrate ion pair was needed to quantitatively describe the catalytic activities. Instead, the results were interpreted entirely in the context of partition rates of the quaternary ammonium ion pairs (i.e., interfacial transport phenomena). As a corollary, the QSAR modeling results indicated that the catalytic activity of tetraalkylammonium ions in reactions with more acidic substrates could potentially be well described by a nonlinear

QSAR model with a single molecular parameter, namely, the thermodynamic partition coefficient of the catalyst.

Thus, a new study was conceived to establish whether the catalytic activity of quaternary ammonium ions was related more to their stoichiometric rate constants or phase transfer rate constants (Scheme 1). The alkylation of phenol was identified as a reaction that would allow for this question to be addressed in a quantitative manner. Described herein is a comparison of the stoichiometric, catalytic, and phase transfer rate constants for a homologous series of quaternary ammonium ion phenolates along with an analysis of their partition equilibria and the composition of the species present in the organic phase.

Scheme 1
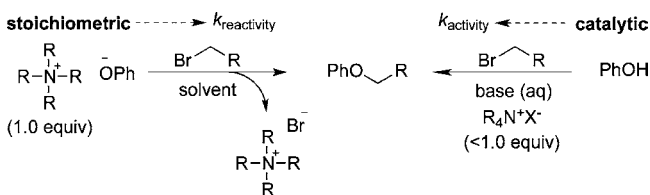
1. Selection of Reaction To Study. The reasons that the alkylation of phenol is the appropriate reaction for this study are not obvious and require explanation. The identification and analysis of catalyst structure−activity relationships for PTC reactions are complicated by the fact that two mechanisms can be operative, extraction and interfacial. Table 1 contains three representative alkylation reactions arranged in order of pK_a of the substrate (lowest to highest), from cyanide ($pK_a = 9.4$)[5] to phenol ($pK_a = 18.0$)[6] to an α-aryl nitrile ($pK_a > 18$).[7] As the pK_a of the substrate increases, the dominant operative mechanism shifts from an extraction mechanism where the bond-forming reaction occurs in the organic phase, to an interfacial mechanism where the bond-forming reaction occurs from an interfacially adsorbed ion pair.[8,9]

Table 1. Representative Extraction and Interfacial Phase Transfer Catalyzed Reactions

pKa (DMSO)	reaction	PTC conditions	Mechanism
9.4	N≡C⁻ Na⁺ (aq.) → N≡C–R (conditions)	Octyl₄N⁺Br⁻ (0.01 equiv) R-Cl (XS, liquid)	extraction
18.0	Ph–OH → Ph∼O∼R (conditions)	Bu₄N⁺Br⁻ (0.05 equiv) RCH₂-Br (1-2 equiv) NaOH (1M-18 M, aq.) toluene or CH₂Cl₂, rt	either extraction or interfacial
14-24	Ph∼C≡N → Ph∼C≡N / Et (conditions)	Et₃BnN⁺Br⁻ (0.05 equiv) Et-Cl (1-2 equiv) NaOH (1M-18 M, aq.) benzene, rt	interfacial

To systematically probe catalyst structure−activity relationships for reactions following either an extraction or an interfacial mechanism, it would be most convenient to study a single reaction where the dominant mechanism can be affected by changing the reaction conditions. The alkylation of phenol uniquely fulfills this requirement. For this reason, the alkylation of phenol was identified as a reaction for which a comparison of the stoichiometric and catalytic rate constants as a function of a homologous series of ammonium counterions could serve to bridge the gap of understanding of the two mechanistic regimes of PTC. Our results and analysis for a

phenol alkylation operating under the extraction mechanism are described herein.[10]

2. Mechanisms of PTC.[11] *2.1. Extraction Mechanism of PTC.* In the simplest PTC process, a water-soluble nucleophile such as sodium cyanide reacts by the mechanism outlined in Figure 1.[12] The observed catalytic effect is the physical extraction (or transfer) of the anionic nucleophile to the organic phase (K_2) and thus is termed the "extraction mechanism". In the extraction mechanism, the substrate anion (NC⁻) and product anions (X⁻) are formally distributed between the aqueous and organic phases as quaternary ammonium (Q⁺) ion pairs. The irreversible, bond-forming reaction (k_3) occurs in the organic phase and is the rate-determining step.[12,13] Lipophilic catalysts tend to perform better than hydrophilic ones. Some modifications have been proposed to account for the activity of catalysts that have no appreciable aqueous solubility,[14] but in general, this mechanistic outline has been supported by numerous subsequent investigations.[15]
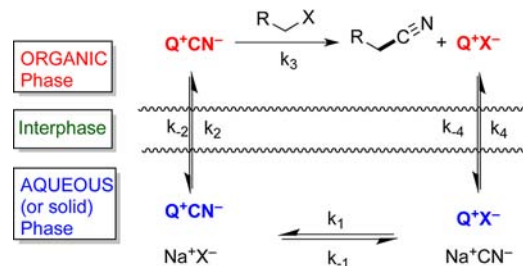

Figure 1. Extraction mechanism of phase transfer catalysis.

2.2. Hydroxide-Initiated PTC. The second example in Table 1 is the alkylation of phenol ($pK_a = 18$) under biphasic conditions in the presence of an aqueous hydroxide base. The use of a neutral substrate in combination with an aqueous base under PTC conditions is termed "hydroxide-initiated PTC".[16] The mechanism of hydroxide-initiated PTC reactions is more complex than the extraction mechanism and involves distinguishing (1) where the substrate is deprotonated, (2) whether the catalyst is involved in the deprotonation step, (3) where the substrate·ammonium ion pair is generated, and (4) how the substrate·ammonium ion pair is transferred to the organic phase.[8b,9,15b,17] Typically, an in situ deprotonation only adds pre-equilibrium steps to the catalytic cycle (K_1 and K_2, Figure 2), and the PTC alkylation of phenols comports with this model.[18,19] As expected, the deprotonation step (k_2) is fast since the pK_a of phenol is much less than that of water ($pK_a =$
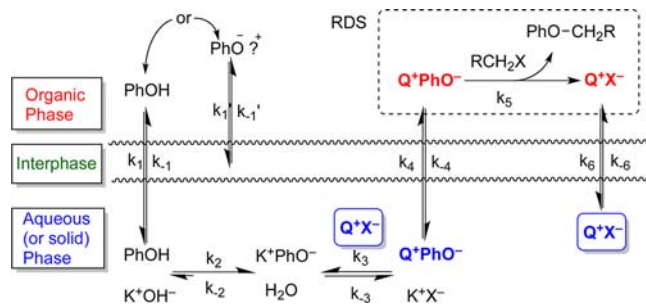

Figure 2. Schematic representation of the hydroxide-initiated PTC alkylation of phenols.
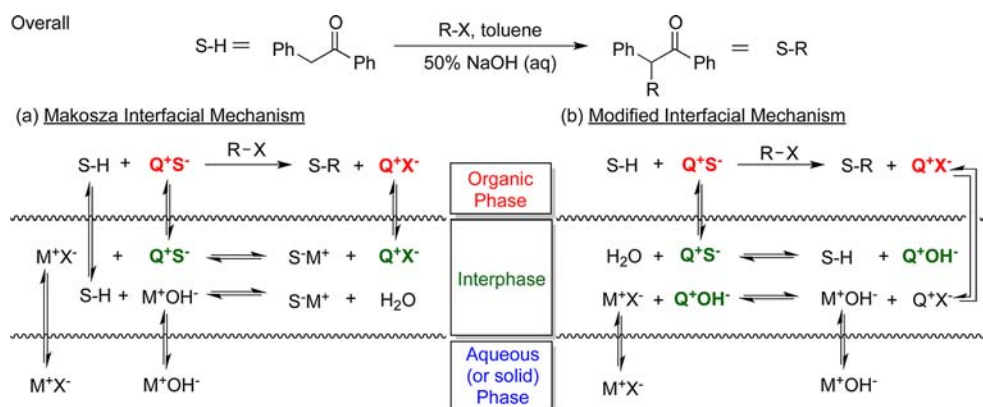
Figure 3. Schematic representation of the interfacial mechanism(s) of phase transfer catalysis: (a) the Makosza interfacial mechanism and (b) the modified interfacial mechanism.

32).[20] However, considerable evidence has been accumulated indicating that "other complicating factors" may become important in the PTC alkylation of phenols, depending on reaction conditions.[21] For example, the formation of a "third liquid phase" (TLP) at the aqueous/organic interface (K_1', Figure 2) has been proposed.[21d] One study reports the purposeful engineering of a TLP (termed "liquid−liquid−liquid PTC") by the addition of sodium chloride (25% by mass) to the aqueous phase.[22] In this way, a stable, reproducible TLP is generated with the relative volumes of organic/TLP/aqueous = 50/4/55 cm³. However, the composition of the TLP during the reaction and consequent mechanistic implications remain largely unknown.

Because of the ambiguity about the exact nature of the space between the organic and aqueous phases under PTC conditions, the terms "interfacial space" and "interphase" will be used throughout this disquisition. To summarize, the alkylation of phenol is sufficiently well-behaved to be explained by the extraction mechanism, but some subtle characteristics of this reaction class can arise from interfacial adsorption/desorption equilibria (K_1', Figure 2). In the present study, the reaction conditions were chosen to ensure PTC catalysis under the extraction mechanism.

2.3. Interfacial Mechanism. The third example from Table 1 is the hydroxide-initiated PTC alkylation of an α-aryl nitrile (18 < pK_a < 25), which is meant to be representative of enolate alkylations.[23a,b] The inability to explain the behavior of hydroxide-initiated PTC reactions of this type by the extraction mechanism led Makosza to propose an interfacial mechanism (Figure 3a).[23c] In the initially proposed interfacial mechanism, the substrate (S−H) and quaternary ammonium catalyst are in equilibrium between the organic phase and the interfacial region. Similarly, the inorganic base (M⁺OH⁻) is in equilibrium with the aqueous phase and the interfacial region. The inorganic base facilitates deprotonation of the substrate, which may then exchange with the quaternary ammonium (Q⁺) to generate the key active species (S⁻Q⁺). The substrate·ammonium ion pair then dissociates from the interface into the organic phase where it may react. Subsequent kinetic studies have shown that quaternary ammonium ions can influence the rate of substrate deprotonation,[24] which provides support for a second, modified interfacial mechanism (Figure 3b).[9] The major modification is that the quaternary ammonium halide (Q⁺X⁻) is in equilibrium with the quaternary ammonium

hydroxide (Q⁺OH⁻), which acts as the base that actively deprotonates the substrate.

■ BACKGROUND

1. Analyses of Catalyst Structure−Activity Relationships for Extraction PTC Reactions. One of the most thorough studies in support of the extraction mechanism of phase transfer catalysis compared the catalytic activity of 13 straight-chain quaternary ammonium and phosphonium ions under stoichiometric, homogeneous (1.0 equiv) and catalytic, heterogeneous (0.1 equiv) phase transfer conditions.[14d] In that study, comparison was made between the rates of displacement of methyl octyl sulfonate with small, hydrophilic, weakly basic nucleophiles including Cl⁻, Br⁻, I⁻, SCN⁻, N₃⁻, and CN⁻ (Scheme 2, top).

Scheme 2
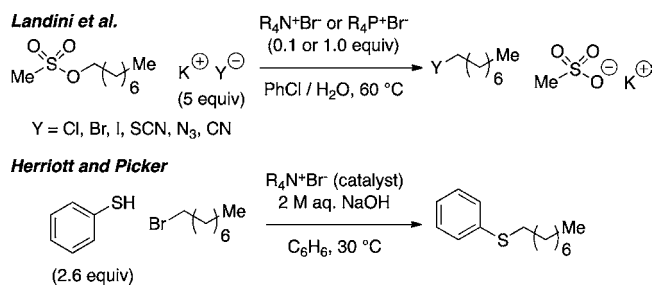
Under PTC conditions the observed rate constants differed by up to 2 orders of magnitude between different ammonium ion catalysts. Under homogeneous conditions the observed rate constants differed by only a factor of 2.5. Some attempts have been made to conduct similar studies with more basic substrates. For example, the catalytic activities of 13 quaternary ammonium bromides have been determined for the alkylation of thiophenoxide (Scheme 2, bottom).[14c] Unfortunately, attempts to compare the stoichiometric rate of reaction to those under PTC conditions were complicated by irreproducibility of the alkylation of tetrabutylammonium thiophenoxide in homogeneous media.

In those studies the catalyst activity increased linearly with lipophilicity (log P), but no optimum was identified. Both studies concluded that "the effectiveness of a phase transfer catalyst depends mainly on its organophilicity, with other structural factors [being] much less important."[14c] Thus, the

dominant effect of the catalyst is to increase the effective concentration of the nucleophile in the organic phase. Given the range of substrates studied thus far, it seems plausible that for any PTC reaction operating under the extraction mechanism, the same dominant effect of the catalyst will be observed.

By contrast, in our previous reports on interfacial PTC,[4] as much as a 3.8 order of magnitude rate enhancement was attributed to effective concentration, but *the correlation was not linearly related to lipophilicity (ClogP)*. This study is designed to determine the range of catalyst activity over which a linear relationship with catalyst log P holds, and whether an optimum catalyst lipophilicity can be identified.

**2. Structure−Reactivity Relationships of Phenolates.** The stoichiometric reactivity of phenoxides has been studied extensively.[25] In fact, recognition of the relationship between the acidity and reactivity of substituted phenols is partially responsible for the original concept of the free energy relationship.[6] Alkylation rates of substituted sodium and potassium phenoxides increase when the pendant groups are electron donating ($\rho = -1.1$).[26] These data are consistent with the intuitive notion that, for ion pairs, the greater the charge separation, the more reactive the anionic species will be, and that the charge separation is greater for ammonium phenoxides than for alkali metal phenoxides.[27] The relative reactivities of tetrabutylammonium and potassium phenoxide have been compared by determining the first-order rate constants of alkylation with 1-bromobutane in multiple solvents (DMF, CH_3CN, dioxane).[28] A decrease of 10^3 in rate constant is observed upon changing from dimethylformamide to acetonitrile to dioxane for the alkylation of potassium phenoxide. In contrast, the rates of alkylation of tetrabutylammonium phenoxide, under the same series of reaction conditions, varied by only a factor of 6. Interpolation and molecular modeling have expanded upon these observations. It has been suggested that the effective ionic radii of quaternary ammonium ions increases in the homologous series $Me_4N^+ \approx 2.85$ Å, $Et_4N^+ \approx 3.48$ Å, $(n\text{-}Pr)_4N^+ \approx 3.98$ Å, $(n\text{-}Bu)_4N^+ \approx 4.37$ Å, after which point there is little or no change.[29,30] Not enough data are available to ascertain the certainty of this proposal or how relevant it is to PTC reactions with substoichiometric amounts of quaternary ammonium ion catalysts. However, the analysis is consistent with many of the stoichiometric extractive alkylation studies by Brändström, wherein no catalyst turnover is required.[31]

3. Phase Transfer Catalyzed Alkylation of Phenols. The initial report on hydroxide-initiated PTC alkylations of phenol revealed that a wide range of phenol derivatives and electrophiles (alkyl halides and sulfonate esters) could be employed (Scheme 3).[19]

Nearly all of the reported extensions of this preliminary study focus on preparative aspects[32] but also reconfirm the first-order kinetic behavior in both reacting components as well as the catalyst.[18] A *tour de force* application of kinetic modeling to the study of phenol alkylations has yielded a bounty of insights, but only tetrabutylammonium or benzyltributylammonium cations
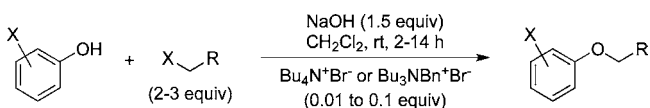
were included.[33] The most recent investigations focus on the generation of a TLP because when a TLP does form it is accompanied by a significant rate enhancement.[34,35] Depending on the conditions, up to 3 orders of magnitude in rate enhancement accompanies the formation of a TLP, which is highly dependent on the organic solvent and ionic strength of the aqueous phase, but the effect of the quaternary ammonium ion structure has not been extensively investigated. Thus, no data are available that are suitable for application of QSAR methods.

4. Solid-State and Solution Structural Data Relevant to PTC Alkylation of Phenols. The study of the solid-state structure and solution-state reactivity of phenols and phenoxides is extensive.[36] In the solid state, most alkali metal phenoxides form extended aggregates with multiple bridging $(O-M-O)_n$ linkages where the number of oxygen−metal contacts varies from 2 to 4 ($\mu_2-\mu_4$).[37] Characterization by single-crystal X-ray diffraction is rare, and most of the solid-state structural data for phenolates are derived from X-ray powder diffraction data.[38] A few exceptions are known wherein cation complexing agents, such as 18-crown-6,[39] or sterically bulky groups have been incorporated[40] to facilitate the collection of single-crystal X-ray diffraction data.

Numerous studies on the pK_a of phenol derivatives have been conducted.[41] The effect of substitution is enhanced in dipolar aprotic solvents ($\rho = 5.3$, DMSO) compared to protic media ($\rho = 1$, H_2O).[6] A complicating factor in studying the reactivity differences of phenol derivatives is the formation of dimeric species in solution (Scheme 4). The dimeric species, termed homo-hydrogen-bonded complexes, are significantly slower to deprotonate than the parent, uncharged phenol derivatives. Thus during the course of a titration, the acidity of the dominant species in solution can change.[6]

Scheme 4

homo-hydrogen bonded complex
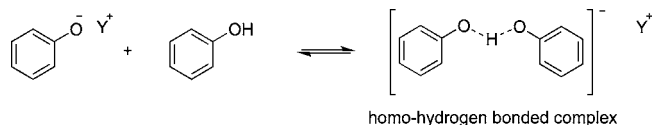
The decreased acidity of homo-hydrogen-bonded phenolate complexes compared to phenols has been exploited in the study of the kinetics of proton transfer reactions. Nielsen and Hammerich described the preparation of the homo-hydrogen-bonded complex $Bu_4N^+[PhOHOPh]^-$ (Scheme 5).[42] Reetz and Goddard modified the procedure for the preparation of X-ray-quality crystals of the same complex.[43]
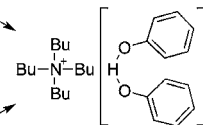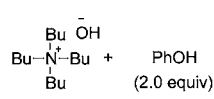
The solid-state X-ray diffraction data show that the closest contact between the ammonium ion α-CH atoms and the anionic phenoxide complex is 2.73 Å, and the average distance

Scheme 3

Scheme 5
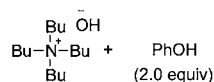
is 3.02 Å. These data are in good agreement with the hypothesis that ammonium cations generate ion pairs that are significantly more separated than alkali metal cations, where analogous bond lengths are significantly shorter (Na, ~2.3 Å; K, ~2.7 Å).[44]

5. Computational Studies on the Structure and Reactivity of Ammonium Salts. The scarcity of structural data for comparison of alkali metal and ammonium ion pairs has provided motivation for a number of computational studies.[45] These studies show that the calculated cation–anion interaction energy is weaker for tetrabutylammonium ion phenolates (2.5 kcal/mol) than for alkali metal cations (Na⁺, 4.5 kcal/mol).[46]

Recently, two types of computational modeling techniques have been applied to the investigation of nucleophile reactivity under catalytic PTC conditions, namely, *ab initio* calculations employing a polarizable continuum solvent model (PCM),[47] and molecular dynamics simulations employing an ensemble of solvent molecules (10−100 molecules).[48] Molecular dynamic simulations suggest that the rate of displacement in a model nucleophilic substitution reaction is highly dependent on the degree of hydration of the nucleophile, which is in turn dependent on where in the interfacial region the reaction takes place. Within 5 Å of the Gibbs surface into the organic phase, the hydration level is still sufficient to mimic the reaction in bulk water. However, beyond this distance the activation barrier continuously decreases as the hydration level decreases. The conclusion is that the role of the PTC is to transport the nucleophile deep into the organic phase such that desolvation leads to increased nucleophilic reactivity.[48]

Similar conclusions have been reached independently by comparison of association constants of quaternary ammonium sulfates in solution, both computationally and experimentally.[49] The computational results suggest that the differences in nucleophilicity of quaternary ammonium ion pairs result from a combination of factors related to solvation, including (1) a decrease in electrostatic interactions between the ions, (2) disruption of dispersion interactions between the anion and the solvent, and (3) generation of solvent cavities in the vicinity of the nucleophile. That is, whereas a greater charge separation may accompany ion exchange from alkali metal to ammonium counterion, the origin of catalytic activity, if any, is more likely a consequence of shielding the nucleophile from protic media, a transition state lowering effect.

6. Objectives of This Study. Thus, it is still unresolved what the nucleophile activation and nucleophile extraction contribute to the net catalytic activity of phase transfer catalysts. The central aim of this study is to determine which relationship best describes phase transfer catalyst activity, a rate–rate (nucleophile activation) linear free energy relationship (LFER) or a rate–equilibrium (nucleophile extraction) LFER. The method chosen was to compare the catalytic rate constant ($k_{activity}$) to the stoichiometric rate constant ($k_{reactivity}$) under conditions that are as analogous as possible.

■ RESULTS

1. Stoichiometric Reactivity of Ammonium Phenolates (Rate−Rate LFER). The initial challenge in this project was to identify a general procedure for the preparation of a homologous series of quaternary ammonium phenolates in homogeneous and halide-free form. In previous studies, tetrabutylammonium phenolates were prepared by mixing tetrabutylammonium bromide and sodium (or potassium) phenoxide.[28] No attempt was made to purify the ammonium

phenolate itself, or to separate the alkali bromide salt from the reaction mixture. The alkali halide contaminant is known to influence the rates of phase transfer catalyzed phenol alkylations.[22,50] Thus, some ambiguity remains about the previous kinetic analyses and mandates that samples of known purity be employed in this study.

1.1. Preparation of Tetraalkylammonium Hydroxides. On the basis of our previous results and known data on PTC cyanide alkylations, it was decided to limit the survey of quaternary ammonium salts to R = Me, Et, *n*-Pr, *n*-Bu, *n*-Hex, and *n*-Oct. To prepare the phenoxides in pure form required the preparation of the corresponding ammonium hydroxides in pure form, as no subsequent purification would be possible. The requisite quaternary ammonium hydroxides were prepared from their bromides by ion exchange, closely following the protocol of Harlow, Noble, and Wyld, with the exception that anhydrous methanol was used as the solvent rather than isopropanol (Table 2).[51] Multiple passes (3−6) through an Amberlyst A-26 resin were required to fully exchange the halide for hydroxide.[52] After each pass, the hydroxide form was regenerated by rinsing the column with a large excess of sodium hydroxide. Sodium hydroxide was chosen because any residual sodium is expected to be less detrimental to the kinetic analyses than potassium. The resulting quaternary ammonium hydroxide solutions were titrated for total base to a phenolphthalein end point (3−6 determinations) and titrated for residual halide with an ion-selective electrode (2−3 determinations).[53] The results for the preparation of the quaternary ammonium hydroxide solutions are shown in Table 2. The final solutions were diluted (or concentrated) such that the total base concentration was between 0.1 and 0.7 M and stored as such. The extent of exchange was greater than 97% in all cases, and the salts could be stored at −20 °C for an extended period (~1 month) with no detectable change in total base titer.

Table 2. Preparation of Quaternary Ammonium Hydroxides in Methanol

entry	ammonium cation	OH conc, [M][a]	std dev	Br, wt %[b]	Br, mmol %[d]
1	methyl₄N⁺	0.127	0.0095	0.16	1.56
2	ethyl₄N⁺	0.668	0.0014	0.33	0.61
3	*n*-propyl₄N⁺	0.229	0.0050	0.34	1.82
4	*n*-butyl₄N⁺	0.588	0.0054	<0.1[c]	<0.10
5	*n*-hexyl₄N⁺	0.685	0.0096	0.31	0.56
6	*n*-octyl₄N⁺	0.426	0.0013	0.41	1.19

[a]Total base titrations are an average of 3−6 determinations to a phenolphthalein end point. [b]Bromide weight percentage is an average of 2−3 determinations by ion-selective electrode. [c]Prepared from the quaternary ammonium iodide, and no residual iodide could be detected. [d]The total mmol of anions is taken as the mmol of hydroxide plus the mmol of bromide.

*1.2. Preparation of Tetraalkylammonium Phenolates.* A number of orienting experiments were carried out to generate monomeric ammonium phenolates of the type R₄N⁺PhO⁻, but none were successful. Preliminary tests for stability with the tetraethylammonium counterion revealed that Et₄N⁺PhO⁻, once generated in anhydrous form, was stable as a solid for only ~8−10 h in a glovebox. Thus, to enable the study of the

stoichiometric reactivity of ammonium phenolate complexes, we resorted to the preparation and evaluation of homo-hydrogen-bonded complexes.[42,43]

A variety of solvents were initially surveyed for the formation of tetraalkylammonium phenolate·phenol complexes including hydrocarbons (hexanes, cyclohexane), aromatic hydrocarbons (benzene, toluene), halogenated (dichloromethane, dichloro-ethane), polar aprotic (THF, dioxane, acetonitrile), and polar protic (methanol, ethanol, isopropyl alcohol) solvents. Ultimately, dioxane proved superior because of several advantageous physical properties. First, its relative high melting point (11−12 °C) allowed for the tetraalkylammonium phenolate solutions to be conveniently stored in a frozen dioxane matrix. Although prolonged storage was never attempted, no signs of decomposition were observed after storage overnight by ^{1}H NMR analysis. Second, dioxane forms substantive azeotropes with water (dioxane/water, 49/51)[54] and methanol (dioxane/methanol, 77/23),[55] as well as ternary mixtures,[56] which allowed for removal of methanol from the salts.

Thus, the methanolic, quaternary ammonium hydroxide solutions were combined with dioxane solutions of phenol to afford quaternary ammonium phenoxides as homo-hydrogen-bonded complexes, $R_4N^+[(PhOH)OPh]^-$. Three azeotropic concentrations from dioxane afforded the tetraalkylammonium phenolate complexes ($R_4N^+[(PhOH)OPh]^-$) as finely pow-dered solids that could be handled in a glovebox. The stoichiometry of the ammonium phenoxide complexes was determined by quenching a small sample into an acetonitrile solution containing a large excess of benzyl bromide and a standard (Table 3). After stirring the alkylation overnight, the relative amounts of phenol and benzyl phenyl ether were determined by gas chromatography (GC). In all cases the stoichiometry was found to be 1:1 (±0.04).

Table 3. Preparation of Quaternary Ammonium Phenoxides as Hydrogen-Bonded Dimers
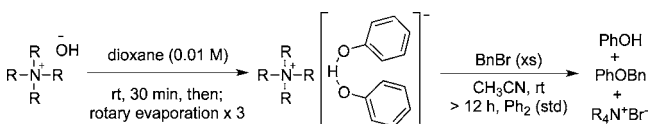
entry	R	PhOH/PhO⁻, mol/mol
1	methyl	1.04
2	ethyl	0.98
3	n-propyl	1.02
4	n-butyl	1.00
5	n-hexyl	0.94
6	n-octyl	0.98

1.3. Stoichiometric Reactivity of Ammonium Phenolates. The reactivity of the tetraalkylammonium phenoxides was determined by employing conditions directly analogous to the most comprehensive set of data available, namely, reaction with a slight excess of 1-bromobutane in acetonitrile at 0.016 M.[28] The least polar, aprotic solvent that was tested and could completely dissolve the tetraalkylammonium phenoxides was diisopropyl ketone (DIPK).[57] Initial-rate kinetic data were collected for each ammonium phenoxide as well as the corresponding sodium and potassium homo-hydrogen-bonded dimers in each solvent (Figure 4). The data from these alkylation reactions have been normalized to the slowest

phenoxide substrate, sodium phenoxide in DIPK (rate for $Na^+[(PhOH)OPh]^- = 5.09 \times 10^{-8}$ mol L^{-1} s^{-1}).[58]
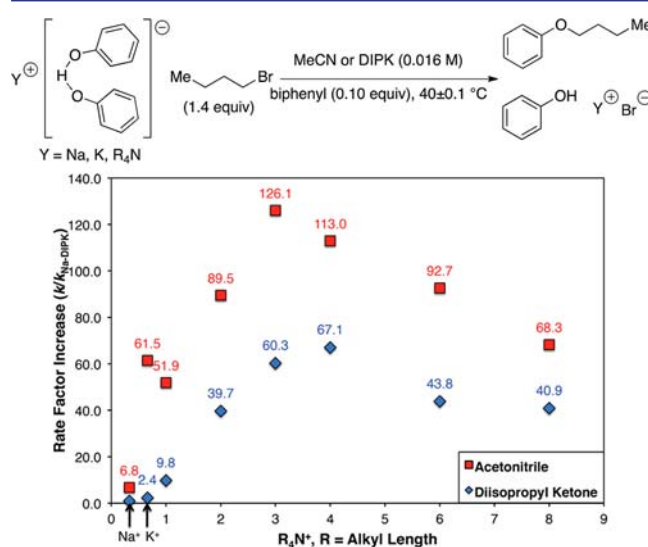

Figure 4. Tetraalkylammonium phenoxide alkylation rates (stoichio-metric).

The reactions were monitored to typically 5−10% conversion, and reaction rate is expressed as the mean of triplicate reactions in terms of the change in *n*-butyl phenyl ether concentration (mol/L) with respect to time (s).[59] The error bars in the summary plot represent one standard deviation in reaction rate. Reactions performed in acetonitrile were between a factor of 1.5 and 5 faster than those in DIPK for all of the quaternary ammonium cations examined. Overall, the reaction rates were more reproducible in DIPK than in acetonitrile, perhaps because of the difficulty of removing all adventitious water from the acetonitrile.

The rates of alkylation of the various phenoxide salts exhibited a modest solvent dependence; DIPK displayed a wider range in rate (a factor of 67.0) compared to acetonitrile (a factor of 18.6). Closer inspection of the data reveals that the greatest difference in rates was seen for the alkali metal (Na^+ and K^+) or Me_4N^+ cations. For acetonitrile, the alkylation rate for the potassium phenoxide ($K^+[(PhOH)OPh]^-$) was 9-fold faster than that for the sodium phenoxide ($Na^+[(PhOH)-OPh]^-$), whereas in DIPK, the rate of alkylation of the potassium salt was only 2-fold greater that that of the sodium salt. Curiously, the alkylation rate of $K^+[(PhOH)OPh]^-$ was 1.2-fold *faster* than that of $Me_4N^+[(PhOH)OPh]^-$ in acetonitrile, whereas it was 4-fold *slower* than the rate for $Me_4N^+[(PhOH)OPh]^-$ in DIPK.

Within the series of homologous tetraalkylammonium salts, the range in rate was remarkably small. In acetonitrile the rates varied by a factor of only 2.4; the highest reaction rate was observed for $(n\text{-}Pr)_4N^+$. In DIPK, the rates varied by a factor of 6.8, with the highest rate observed for $(n\text{-}Bu)_4N^+$. The largest rate effect was the difference in reactivity between Me_4N^+ and Et_4N^+; in acetonitrile the difference was small (1.7-fold faster for Et_4N^+), whereas in DIPK a larger difference was observed in (4.0-fold faster for Et_4N^+).

This finding suggests that, for phenoxide alkylations, the effective ionic radius of quaternary ammonium cations is not highly variable. The stoichiometric reactivity of the surveyed quaternary ammonium cations had a poor correlation to their

cationic radii in the respective tetraalkylammonium phenoxide ion pair.

2. Catalytic Activity of Ammonium Phenoxides under Phase Transfer Conditions. The catalytic activity of the same series of quaternary ammonium cations was evaluated under directly analogous conditions (40 °C, DIPK, 0.27 M in n-BuBr) starting from the quaternary ammonium bromide. Several aqueous base concentrations were tested (10 M and 50% (w/w) aqueous NaOH and KOH), and it was observed that 5 M aqueous KOH afforded the most reproducible results. Both phases appeared homogeneous prior to and after the addition of n-butyl bromide at ambient (~20 °C) and elevated temperatures (40 °C). The initial rate for the formation of n-butyl phenyl ether was monitored by GC analysis.[59]

Under these reactions conditions, the background reaction was very slow; only 5% conversion to product was observed after 5 days (Figure 5).[60] All of the catalysts were evaluated at 0.05 equiv loadings and in addition at 0.10 equiv loadings for $(n\text{-Pr})_4N^+Br^-$ (TPAB), $(n\text{-Bu})_4N^+Br^-$ (TBAB), $(n\text{-Hex})_4N^+Br^-$ (THAB), and $(n\text{-Oct})_4N^+Br^-$ (TOAB).
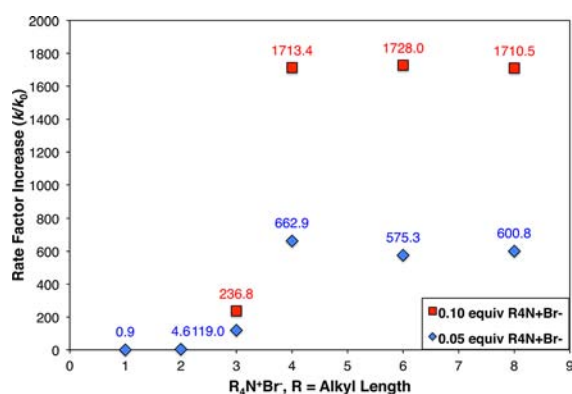

Figure 5. Catalyst survey for PTC phenol alkylation.

Tetramethylammonium bromide (TMAB) was found to be an inactive catalyst at 0.05 equiv loading and afforded an alkylation rate no greater than the background rate. At the same catalyst loading, tetraethylammonium bromide (TEAB) was able to catalyze the reaction 4.6 times faster than background, and TPAB catalyzed the reaction 167 times faster than background. Another significant jump in catalytic activity was observed with TBAB, which afforded a 663-fold rate increase over background, the maximum rate observed for the series. For salts more lipophilic than TBAB, only small changes in catalytic activity were seen at 0.05 equiv. Virtually no difference was seen among these salts at 0.10 equiv loading as well (Figure 5).

The range in catalytic activity among the homologous tetraalkylammonium salts (a factor of 663) was approximately 100-fold greater than the range in reactivity observed for $R_4N^+[(PhOH)OPh]^-$ under homogeneous reaction conditions (a factor of 6.8). A relatively large difference in catalytic activity was seen with TEAB and TPAB under PTC reaction conditions (25.9-fold) in contrast to the homogeneous reaction conditions that displayed similar reactivities with the same cations (1.5-fold). As was the case in the reactions of the tetraalkylammonium phenoxides under homogeneous reaction conditions in DIPK, the maximum rate was observed with the $(n\text{-Bu})_4N^+$ cation. However, in DIPK under homogeneous reaction conditions, the reactivity decreased slightly after TBAB,

whereas under PTC conditions the catalytic activity did not vary for catalysts larger than TBAB. The catalyst survey under PTC reaction conditions clearly demonstrates that the intrinsic reactivity of $R_4N^+[(PhOH)OPh]^-$ has little effect on the observed catalytic activity.

3. Confirmation of Extraction Mechanistic Regime.
3.1. Order in n-BuBr. Although the PTC alkylation of phenols is known to operate by an extraction mechanism,[18b] we are unaware of a case in which such a clearly nonlinear dependence of catalytic activity and catalyst lipophilicity has been reported.[61] A break in an LFER-type plot (see Discussion for detailed LFER/QSAR analysis) has two common interpretations, namely, a change in rate-determining step or a change in mechanism.[62] The clearly nonlinear relationship observed herein prompted us to test if either of these interpretations was the origin of the observed nonlinear dependence of catalytic activity on catalyst lipophilicity.

The possibility of a change in reaction mechanism and rate-determining step was excluded by determination of the reaction order in electrophile. The order in n-butyl bromide was determined by the method of initial rate kinetics for two catalysts (TPAB and TOAB), one on either side of the break in the LFER (Figure 6). Plotting the resultant initial rates versus
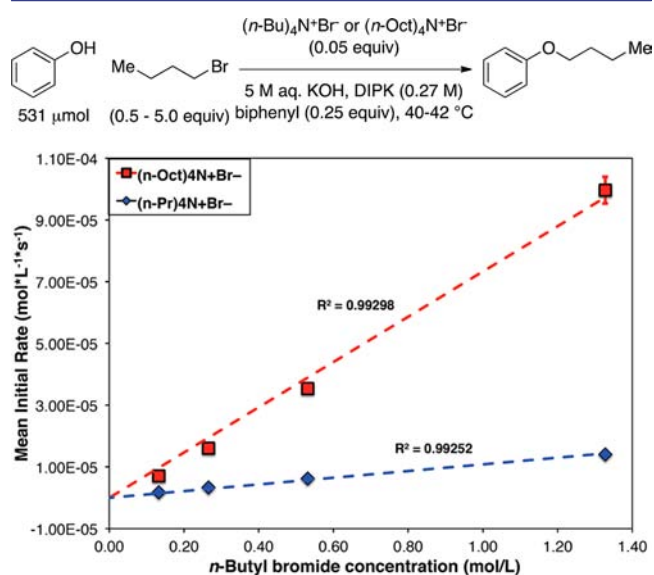

Figure 6. Order in n-butyl bromide for PTC alkylation of phenol.

the concentration of n-butyl bromide (0.5, 1.0, 2.0, and 5.0 equiv with respect to phenol) revealed a linear relationship for both catalysts. This finding is indicative of a pseudo-first-order rate dependence in electrophile under PTC conditions, confirming that the rate-determining step is the bond-forming reaction (k_4, Figure 2).

If a change in reaction mechanism were operative (i.e., a change from intrinsic rate to transport rate limiting), then a different order in electrophile would be observed for the two catalysts. If one of the catalysts led to a transport rate-limited PTC reaction, then a zeroth-order dependence on n-butyl bromide would be expected. We conclude therefore that a change in rate-determining step or mechanism is *not responsible* for the differences in catalytic activity between the ammonium ions. The slope of the linear dependence is strongly dependent on the catalyst employed, indicating that although the catalytic rate is highly dependent on the catalyst, the rate differences do

not arise from changes in the rate-determining step, but rather from differences in the pre-equilibria (k_1, k_2, or k_3, Figure 2).

3.2. Order in Catalyst. Carrying out the alkylation with 0.10 equiv instead of 0.05 equiv of TPAB afforded a 2-fold increase in alkylation rate, consistent with an intrinsic rate-limited PTC reaction that is first order in catalyst. However, a similar doubling of the catalyst loading for TBAB, THAB, and TOAB led to increases in alkylation rate by factors of 2.6, 3.0, and 2.9, respectively. These increases in alkylation rates suggest the presence of higher order phenoxide aggregates in the organic phase (vide infra). The emergence of an interfacial mechanism may also be responsible for the alkylation rate augmentation.

3.3. Effect of Stirring Speed on Alkylation Rate. To determine whether an extraction mechanism or interfacial mechanism was operative, a variable stirring speed experiment was conducted with TBAB as the catalyst.[9,63] The PTC reaction had to be run at ambient temperature because of the design of the electric motor. The stirring speed was varied from 500 to 2000 rpm, and no dependence of the reaction rate on the stirring speed was observed above 500 rpm (Figure 7). Therefore, this result supports an extraction mechanism and an intrinsic reaction rate-limited PTC reaction.
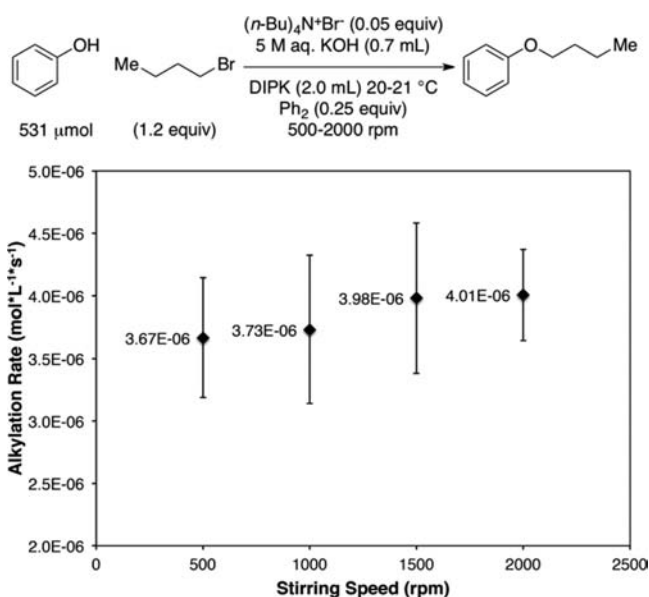

Figure 7. Variable stirring speed under PTC reaction conditions.

All of the data collect thus far are consistent with those found in previous studies and support an intrinsic reaction rate-limited PTC process operating by an extraction mechanism. In the context of a QSAR/LFER analysis of catalysis, the data are most consistent with a third, less common rationale for a break in a LFER plot, namely, a *change in a pre-equilibrium position* and no change in rate-determining step or mechanism.

4. Analysis of Composition of the Organic-Phase Ammonium Phenolate Ion Pair(s). With a change in reaction mechanism ruled out as the origin of the plateau in catalytic activity as a function of ammonium ion size, two pre-equilibria remain wherein the catalyst is necessarily involved, namely, anion exchange (k_3, Figure 2) and equilibration of the ammonium phenolate ion pair between the aqueous and organic phases (k_4, Figure 2). As a corollary, if the composition of the extracted ammonium phenoxide species varied system-

atically, this too could be the origin of the differences in catalytic activity of the ammonium ions.

A priori, the phase partition equilibrium (k_3) seemed to be the most logical source of the trend because partition coefficients, P (in this case $P = K_3 = k_3/k_{-3}$), are known to be directly proportional to the number of carbons in the partitioning,[64] while many known ionic equilibria of ammonium ions are known not to be highly dependent on the ammonium ion.[27] Nonetheless, we sought to collect a set of data to (1) show that the amount of extracted ammonium phenolate increased along the homologous series of ammonium ions and (2) analyze the composition and stoichiometry of the extracted ammonium phenolate ion pairs. Several experiments were conducted to quantify the amount of this reactive species in the organic phase.

4.1. UV−Vis Spectroscopic Analysis of the Aqueous Phase. The first series of experiments is designed to analyze the pre-equilibrium partitioning of phenol/phenoxide (k_4, Figure 2), which could readily be analyzed by UV−vis spectroscopy. The greatest shortcoming of this analysis is that the concentration in the organic phase had to be determined by difference, because the DIPK (organic phase solvent) is UV-active and its absorption is coincident with the UV absorption of phenoxide. Therefore, in this study, the concentrations of phenol/phenoxide in the *aqueous phase* were used to calculate the amount of phenoxide transferred to the organic phase. The same tetraalkylammonium bromides were analyzed by this method for the amount of phenoxide transferred to the organic phase under catalytic conditions employing substoichiometric (0.2 equiv) and stoichiometric (1.0 equiv) amounts of the ammonium salts.

The results from this series of experiments (Figure 8) show that the more lipophilic ammonium ions extracted more of the
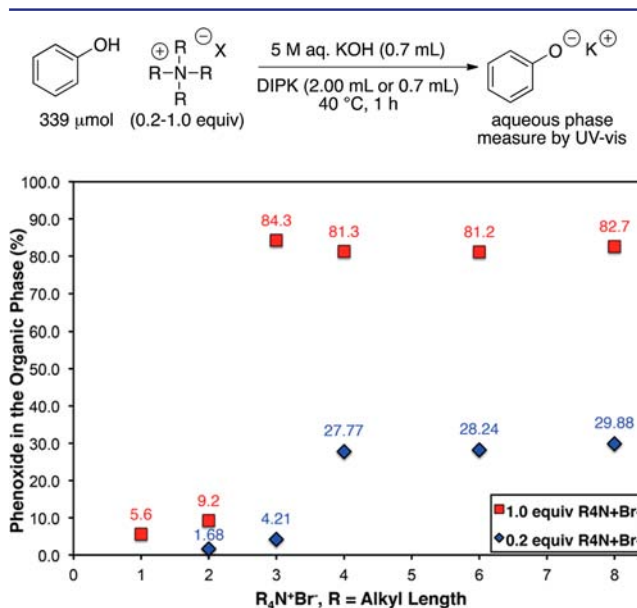

Figure 8. Composition of phenol in the organic phase by UV−vis analysis.

phenol/phenoxide to the organic phase, as expected. With 1.0 equiv of the tetraalkylammonium bromides, the more lipophilic salts, TPAB to TOAB, transferred a large amount of phenoxide to the organic phase, whereas the less lipophilic salts, TMAB and TEAB, transferred only a small amount of phenoxide.

Similarly, when 0.2 equiv of the ammonium salts was employed, the same trend was observed with the exception that the relative amount of phenol extracted by TPAB decreased significantly.

Notably, when a stoichiometric amount of TPAB was employed, an amber-colored TLP was observable between the aqueous and organic phases (Figure 9). Analysis of the TLP
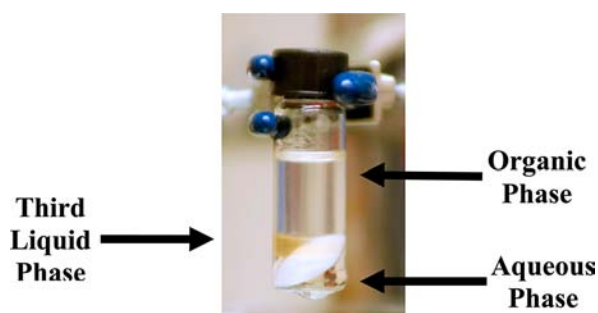

Figure 9. Third liquid phase visible with 1.0 equiv of TPAB.

by UV–vis spectroscopy indicated that the phenoxide concentration was a little more than twice the starting aqueous phase concentration.[65] In contrast, at 0.2 equiv catalyst loading, a large difference in phenoxide transport was observed between TEAB and TBAB (a factor of 16.5). The largest difference was seen between TPAB and TBAB, which afforded nearly a 7-fold increase in the transport of phenoxide out of the aqueous phase. At 0.2 equiv of TPAB, the amount of transferred phenoxide was drastically reduced, and no TLP was observed. Taking into account the relatively large alkylation rate observed for TPAB (a factor of 120 over background), this finding suggests that the observed TLP is rich in both ammonium and phenoxide ions. The critical catalyst concentration required for the formation of TLP with TPAB was not determined.

Perhaps the most startling finding of the survey of phenoxide extraction coefficients as a function of tetraalkylammonium ion was that the amount of phenol transferred to the organic phase could be greater than the amount of ammonium bromide employed! *With only 0.2 equiv (20 mol %) of tetraalkylammonium bromides, 27.2%, 27.6%, and 29.3% of the available phenoxide was transferred to the organic phase for TBAB, THAB, and TOAB, respectively.* This corresponds to a greater than 100% transfer of phenoxide per molecule of tetraalkylammonium salt. This striking discovery necessitated a direct analysis of the composition of the organic phase to confirm such an unexpected outcome.

4.2. Titration of Active Phenoxide in the Organic Phase. The second series of experiments involved careful quantitative analysis of the amount of phenoxide transported to the organic phase. This determination was accomplished by allowing the aqueous and organic phases containing phenol and tetraalkylammonium bromide to reach equilibrium, removing precisely measured aliquots from the organic phase, and quenching these aliquots with an excess of benzyl bromide. The quenched reaction aliquots were analyzed for both phenol and benzyl phenyl ether by GC with the aid of biphenyl as an internal standard. The same tetraalkylammonium salts were surveyed at 0.1 equiv with respect to phenol (Figure 10).

The results presented in Figure 9 qualitatively confirm the striking conclusion from UV–vis spectroscopy. The hydrophilic ammonium salts, TMAB, TEAB, and TPAB, transferred only traces of phenoxide to the organic phase; in fact, more neutral
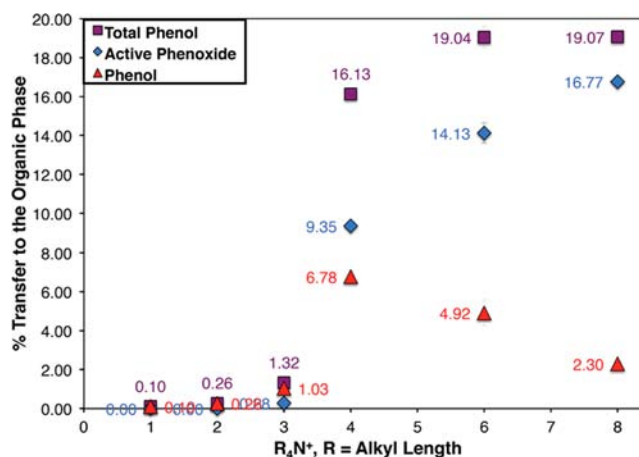

Figure 10. Composition of phenol in the organic phase by titration.

phenol was found than phenoxide. However, the more lipophilic ammonium salts transferred stoichiometric (TBAB, 9.35%) and superstoichiometric (THAB, 14.13%; TOAB, 16.77%) amounts of phenoxide to the organic phase. Moreover, the increasing amount of phenoxide transferred to the organic phase with increasing alkyl chain length is accompanied by a corresponding decrease in the amount of neutral phenol transferred. Thus, the total amount of phenol transferred (black squares) roughly corresponds to the results obtained from the UV–vis spectroscopic analysis, now with finer resolution of the constituent components.

The presence of phenol in the organic phase was unexpected because the use of concentrated aqueous potassium hydroxide should heavily favor (by several pK_a units) the formation of potassium phenoxide at equilibrium. Even more interesting was that the concentration of organic-phase phenol was unique to each ammonium salt examined, and therefore not simply a consequence of the specific base and solvent. For TBAB, THAB, and TOAB, the amount of neutral phenol transferred was found to be 6.78, 4.92, and 2.30%, respectively. The less lipophilic tetraalkylammonium salts transported a greater amount of phenol in the organic phase. The transport of neutral phenol implicates a still more complex aggregate structure wherein phenol may serve to stabilize phenoxide anions by hydrogen bonding.

4.3. Determination of the Amounts of R_4N^+ and K^+ Phenoxide in the Organic Phase. The intriguing observation of superstoichiometric transport of phenoxide to the organic phase was further investigated to determine the relative amount of tetraalkylammonium vs potassium phenoxide being transferred. Experiments to quantify the amount of potassium phenoxide associated with $[R_4N^+PhO^-]$ in the organic phase were limited to TBAB, THAB, and TOAB. The protocol for these experiments was the same as for the titrations described in the previous section: 0.10 equiv of the tetraalkylammonium bromide, quenching aliquots of the organic phase with an excess of benzyl bromide. The potassium bromide that was produced in the alkylation was then removed by an aqueous extraction. The potassium concentration of the resulting aqueous solution was determined by inductively coupled plasma optical emission spectroscopy (ICP-OES) (Table 4). The amount of ammonium phenoxide present in the organic phase was calculated as the difference between the transferred *potassium* phenoxide and the *total active phenoxide*, as was determined by the benzyl bromide titrations in section 4.2.

Table 4. ICP-OES Determination of Potassium Concentrations[a]

$R_4N^+Br^-$, R (0.10 equiv)	transfer of K^+PhO^-, % (standard deviation)	$R_4N^+PhO^-$, % in the organic phase
n-Bu	0.41 (0.05)	89.4
n-Hex	4.40 (0.08)	97.3
n-Oct	6.95 (0.70)	98.2

[a]All values shown are the mean of triplicate runs.

For TBAB only a small amount of potassium phenoxide was found in the organic phase. However, 11- and 17-fold increases in the amount of transferred potassium phenoxide were observed for THAB and TOAB, respectively. Additionally, the more lipophilic the ammonium cation, the greater the amount of the quaternary ammonium phenoxide ion pair present in the organic phase. These results clearly show that, for TBAB, THAB, and TOAB, between 89.4 and 98.2 of the available phenoxide is transported to the organic phase. Most importantly, the unexplained surplus of phenoxide seen in both UV−vis analysis and benzyl bromide titrations can be accounted for by transport of potassium phenoxide into the organic phase by THAB and TOAB. Since absolutely no potassium phenoxide is transported to the organic phase in the absence of the tetraalkylammonium salt, these results point to the formation of aggregates containing both tetraalkylammonium and potassium cations.

■ DISCUSSION

1. Comparison of Stoichiometric and Catalytic Systems. *1.1. Stoichiometric Reactivity.* The stoichiometric reactivity and catalytic activity profiles of the quaternary ammonium salts differed significantly. The data collected in Figure 4 reveal a number of important trends. First, the reactivity of all of the tetraalkylammonium phenolates was greater than that of the sodium or potassium phenolates. Second, under homogeneous reaction conditions the range of reactivity of the tetraalkylammonium phenolates varied by a factor of only 2.4 in acetonitrile and 6.8 in DIPK. If only the quaternary ammonium cations larger than Me_4N^+ are compared, then the reactivity range is reduced further to 1.4- and 1.7-fold for acetonitrile and DIPK, respectively. Third, the homo-hydrogen-bonded complexes Et_4N^+, $(n\text{-Hex})_4N^+$, and $(n\text{-Oct})_4N^+$ reacted at nearly identical rates (1.1-fold difference). However, the $(n\text{-Pr})_4N^+$ and $(n\text{-Bu})_4N^+$ complexes reacted at slightly increased rates (1.5 and 1.7 times, respectively).

These data clearly show that the effect of charge separation on rate appears to be small and does not reflect the ionic radii of the corresponding ammonium ions; i.e. an increase in the ionic radius is expected to correlate with an increase in reactivity. However, a structural parameter more relevant to ion pair reactivity is the "closest approach of the ion" (*a*), which reflects the distance between the positive charge of the ammonium cation and the negative charge of the phenolate. The parameter *a* can be estimated by comparing ion pair formation constants (K_{ip}) with predictions form Bjerrum theory. Closest approach parameters have been determined for the quaternary ammonium picrates $(C_nH_{2n+2})_4N^+$ for $n = 1−8$ and are plotted against the relative rates of alkylation in Figure 11.[66] For Me_4N^+ through $(n\text{-Bu})_4N^+$, the reactivity of the phenoxide ion pair correlates well with the closest contact parameter, whereas for $(n\text{-Hex})_4N^+$ and $(n\text{-Oct})_4N^+$ the predicted reactivity deviates. The origin of this deviation is

that the longer alkyl chains in $(n\text{-Hex})_4N^+$ and $(n\text{-Oct})_4N^+$ can introduce a significant entropic component to the transition structure of the alkylation reaction (Price−Hammett principle), thus lowering the rate.[67]
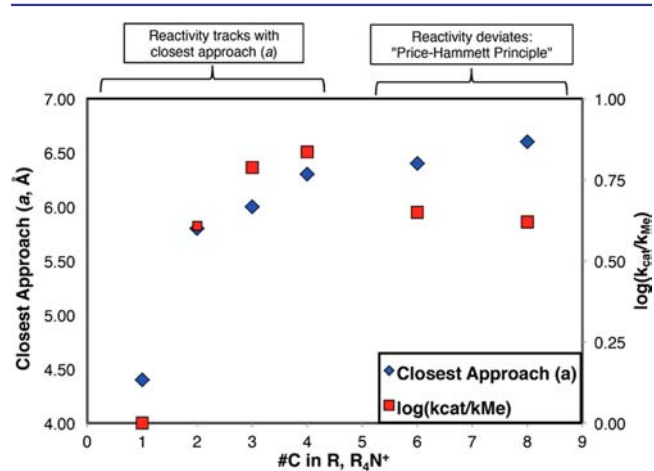

Figure 11. Comparison of relative rates of alkylation closest approach parameter *a*. Extraction constant = $[R_4N^+(\text{picrate}^-)]_{org}/\{[R_4N^+]_{aq}[\text{picrate}^-]_{aq}\}$.

1.2. Catalytic Activity. In contrast, under PTC reaction conditions (in DIPK), from K^+ to $(n\text{-Bu})_4N^+$, the range in reactivity spanned a factor of 663. For quaternary ammonium cations larger than Me_4N^+ in the PTC series, the reactivity range spanned a factor of 144. Thus, by comparison of the stoichiometric and catalytic rates, it is clear that the intrinsic reactivity of the tetraalkylammonium phenoxide ion pair does not contribute significantly to the reactivity of the quaternary ammonium salts under PTC reaction conditions.

In the catalytic cycle, the reactive ion pair, $R_4N^+PhO^-$, is first generated in the aqueous or interphase layer and must traverse into the organic phase for the alkylation to occur. For the $[Me_4N^+PhO^-]$ and $[Et_4N^+PhO^-]$ ion pairs this transport is unfavorable because of their lesser lipophilic character compared to $[(n\text{-Bu})_4N^+PhO^-]$, $[(n\text{-Hex})_4N^+PhO^-]$, and $[(n\text{-Oct})_4N^+PhO^-]$. The tendency for quaternary ammonium salts to enter the organic phase is accurately reflected in their extraction constants. These equilibrium constants have been measured for many different quaternary ammonium salts of varying alkyl lengths and for different gegenions in organic/aqueous biphases.[68] Of relevance to this work, the extraction constants for several quaternary ammonium picrates partitioning between methylene chloride and water were chosen for comparison.[69] Graphical presentation of the log of these extraction constants with the log of rate constant ratios[70] for the PTC reaction shows an excellent correlation (Figure 12). This correlation strongly suggests that the rate of the PTC reaction is dominated by the change in effective concentration of the reactive quaternary ammonium phenoxide in the organic phase.

2. QSAR Analysis of Catalytic Activity.[71] Previous studies have described catalytic activities of tetraalkylammonium ions that span as much as 2−2.5 orders of magnitude in certain PTC reactions. In these studies, the reactions operate by an extraction mechanism, and the catalytic activity is linearly dependent on catalyst lipophilicity, as measured by the number of carbons in the catalyst or the catalyst log P. In our prior investigations, we observed that PTC reactions operating by an
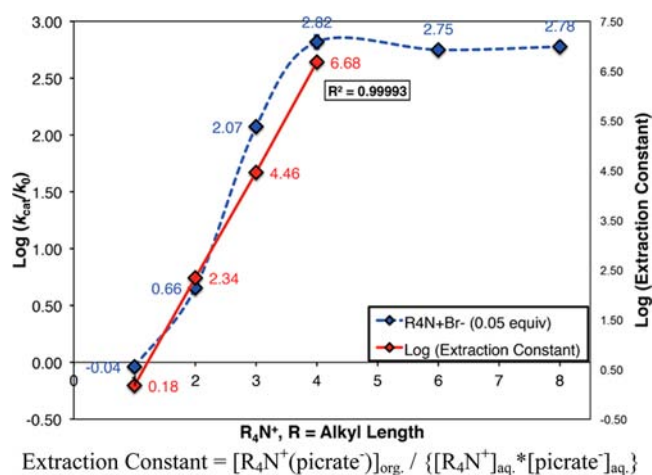
Figure 12. PTC initial alkylation rate with log(extration constant) overlayed.

Figure 13. (a) Plot of the catalytic activity of homologous quaternary ammonium ions vs the number of carbons in each catalyst. (b) Log–log plot of the catalytic activity of homologous quaternary ammonium bromides vs the octanol–water partition coefficient. The black line is a partial least-squares fit of eq 1.

interfacial mechanism exhibit a range of catalytic activity up to 3.8 orders of magnitude. Therefore, it was surprising to observe such a stark break from linearity in the plot of catalyst activity vs catalyst lipophilicity as illustrated in Figure 12.

The data in Figure 11 clearly show a good correlation between catalytic rate and lipophilicity for the smaller ammonium ions (Me_4N^+, Et_4N^+, $(n\text{-}Pr)_4N^+$, and $(n\text{-}Bu)_4N^+$). In this series, the increase in the catalytic turnover frequency is directly proportional to the number of carbons in the ammonium ion catalyst. No further increase in catalytic activity is observed for more lipophilic catalysts. These conclusions can be readily gleaned from a graphical representation that plots log k_{cat} vs either the total number of carbons in the catalyst (Figure 13a) or ClogP (Figure 13b). However, the representation of lipophilicity as the log of the partition coefficient is more valuable, as it lends naturally to interpretation of the data as a rate–equilibrium QSAR. The calculated partition coefficient between octanol and water ($ClogP_{(o/w)}$) is used for the x-axis because computational models for DIPK solvation are not as readily available.

To facilitate analysis by a LFER the data are fitted to a linear biexponential equation (eq 1), with regression statistics $n = 6$, $R^2 = 0.991$, $s = 0.190$. To the best of our knowledge, this is the first application of this kind of analysis in catalysis; therefore, clarification of the parts that make up the fitted equation is warranted.

$$\log(k_{cat.}/k_o) = -\eta \ln[e^{-a(x-x_o)/n} + e^{b(x-x_o)/n}] + c \qquad (1)$$

where $\eta = 0.434$, $x_o = 0.198$, $a = 0.588$, $b = 0.00$, and $c = 2.184$.

The linearized biexponential model, as first proposed by Buckwald, is a useful tool for the analysis of QSAR data showing any type of bilinear distribution.[72] Part of the utility of the linearized biexponential model is the relative ease with which the data are related to the two intersecting LFERs that comprise the bilinear distribution. In this case, the first LFER is reflected in the slope of the regression over the first four data points (blue dashed line, rising slope, $a = 0.588$). This LFER reflects an increase of 0.59 orders of magnitude in catalyst activity per order of magnitude change in the partition coefficient and is also reflected in the bilinear model ($a = 0.588$). The LFER holds until the partition coefficient is near zero, at which point a sharp break is seen and no further change in catalytic activity is observed. The break point, shown in the
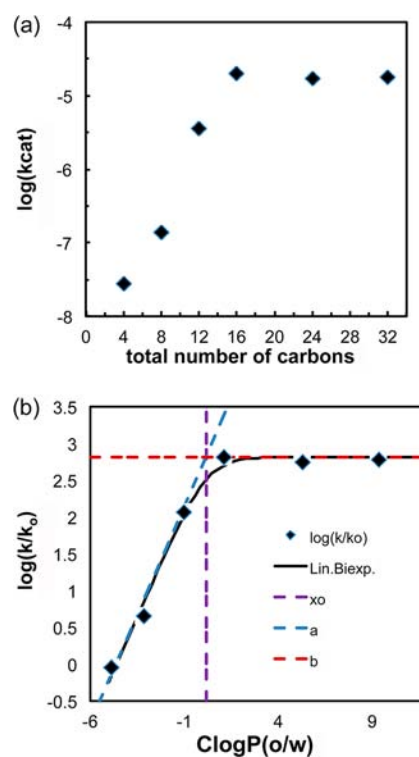
bilinear model as x_o (purple dashed line, $x_o = 0.198$), represents the point of intersection of the two LFERs. The point of intersection indicates that the maximum catalytic turnover frequency is not reached until the catalyst is lipophilic enough to reside predominantly in the organic phase (ClogP > 0). The second LFER is represented by the red dashed line with a slope of zero (descending slope, $b = 0$). Finally, the constant c corresponds to the maximum value of the catalytic data set (on a $\log_{10}$ scale) and is coincident with the red dashed line, i.e., the magnitude of rate acceleration over the background rate. The value of η, which affects the curvature at the intersection of two LFERs, was not varied in the regression analysis. Therefore, η will not be discussed further.

3. Mechanistic Analysis. A break in an LFER-type plot describing reactivity has two common interpretations, namely, a change in rate-determining step or a change in mechanism. However, in studies of catalysis a third possibility exists, namely, a change in a pre-equilibrium position and no change in rate-determining step or mechanism. The data collected to date are most consistent with this third possibility and can be readily interpreted in the context of a continuum of the extraction and interfacial mechanisms.[11] Depending upon the lipophilicity of the tetraalkylammonium salt, several equilibria operate prior to the irreversible alkylation step for hydroxide-initiated PTC reactions that follow an extraction mechanism (Figure 14). For less lipophilic tetraalkylammonium salts the four equilibria involve (1) partitioning of the substrate, (2) deprotonation of the substrate, (3) ion exchange of the potassium and ammonium salts, and (4) partitioning of the ammonium·substrate ion pair into the organic phase ($k_1–k_4$). However, with highly lipophilic salts having negligible water solubility, three

additional equilibria (k_6–k_8) operate at the interface to effect ion exchange of the aqueous phenoxide. As described above, previous studies on the structure−activity relationship of quaternary ammonium ion catalysts for reactions following an extraction mechanism have concluded that the more lipophilic the catalyst (more carbons), the greater will be the activity of the catalyst. No maximum or "leveling-off" of catalytic activity is on record.
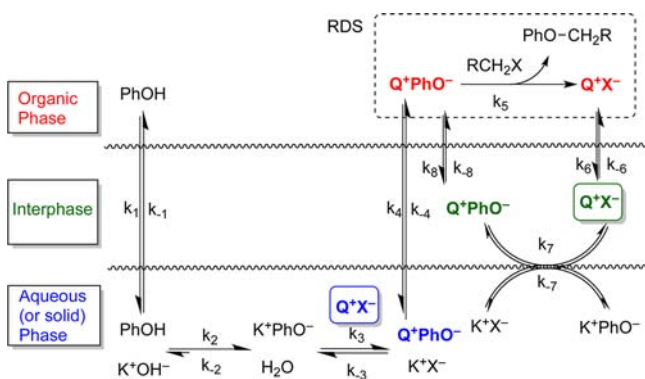

Figure 14. Schematic representation of the hydroxide-initiated PTC alkylation of phenols.

The data collected herein are completely consistent with those studies in that catalyst activity is linearly correlated with catalyst lipophilicity (number of carbons or log P) over a range of ∼2.5 orders of magnitude in catalyst activity. This trend is easily interpreted in terms of a corresponding increase in the concentration of the active species in solution as measured from the titration experiments. However, in the alkylation of phenol no further increase in catalytic activity is observed beyond a rate enhancement of 2.8 orders of magnitude over the background reaction for more lipophilic catalysts (e.g., (n-Oct)$_4$N$^+$ ClogP = 9.56, #C = 32). The observed leveling-off of catalytic activity can also be easily explained by the results from the titration experiments. For the lipophilic quaternary ammonium cations ((n-Bu)$_4$N$^+$, (n-Hex)$_4$N$^+$, and (n-Oct)$_4$N$^+$), the equilibrium concentrations of the reactive species Q$^+$PhO$^-$ in the organic phase (k_8/k_{-8}, Figure 14) reach their maximum obtainable values under these conditions. It is important to note that the extraction constants of the tetraalkylammonium cations have not leveled off, but under these conditions (0.1 equiv of catalyst) the enhanced ClogPs cannot be manifested.[73] The alternative interpretation that the break-point corresponds to a change in rate-determining step is ruled out by the uniform kinetic order of the electrophile on either side of the break point.

4. Analysis of the UV−Vis Spectroscopy and Benzyl Bromide Titration Data. Although the UV−vis spectroscopy data were not able to quantitatively determine the composition of reactive species in the organic phase, they did reveal the superstoichiometric transport of phenoxide species into the organic phase. From the observed aqueous-phase concentrations of phenoxide with (n-Bu)$_4$N$^+$, (n-Hex)$_4$N$^+$, and (n-Oct)$_4$N$^+$, it was determined that ∼50% more phenoxide was transferred to the organic phase than the theoretical maximum as constrained by the ammonium salt loading.

The benzyl bromide titration experiments provided a finer resolution of the composition of the species being transported to the organic phase. Much to our surprise, the aggregate contained a significant quantity of potassium phenoxide and phenol, particularly with the more lipophilic catalysts, and the ratio of active phenoxide to phenol was unique to a particular ammonium salt. These findings are striking for two reasons. First, given the difference in pK_a between water and phenol (15.7 and 9.95, respectively), the observation that any phenol was left protonated was unexpected. In a strongly basic, aqueous medium, phenoxide should be highly favored at equilibrium. However, at the interfacial region of a PTC process, this equilibrium may not be as favorable because the stability of homo-hydrogen-bonded dimers could significantly raise the remaining pK_a as the polarity of the medium decreases. Indeed, Dehmlow and Sasson have observed that quaternary ammonium monoalkoxides of diols exhibit greater lipophilicity (larger extraction constants) than the alkoxides of simple alcohols.[74] This behavior is explained by the formation of an intramolecular hydrogen bond within the mono-deprotonated diol that is absent in the alcohol.

Second, despite the unique phenol/phenoxide ratios among (n-Bu)$_4$N$^+$, (n-Hex)$_4$N$^+$, and (n-Oct)$_4$N$^+$, their PTC initial alkylation rates are nearly identical. This discrepancy implies that, under PTC reaction conditions, the ratio of aggregate components is inconsequential to the reactivity of the ammonium phenoxide. The sole determinant of catalytic activity is the effective concentration of the ammonium phenoxide in the organic phase. In hindsight, this result should not be surprising, given the 25-fold greater rate of reaction of (n-Bu)$_4$N$^+$[(PhOH)OPh]$^-$ compared to K$^+$OPh$^-$ in DIPK. A word of caution is warranted here because the presence of potassium alkoxides in the organic phase need not be innocent in other reactions.

To understand the formation of the potassium/ammonium phenoxide aggregates, a closer examination of the mechanism of ammonium phenoxide transport is required. As an ammonium cation approaches the interphase boundary separating the bulk aqueous and organic phases, its alkyl chains are oriented toward the more lipophilic organic phase due to hydrophobic interactions with the aqueous phase. This conformation change creates a greater charge accessibility of the ammonium center. At the interphase the ammonium phenoxide forms first, and with this increased accessibility, additional potassium phenoxide molecules may complex with the ammonium phenoxide to form a dimeric ion pair. This ion pair is highly charged, and without sufficient lipophilicity provided by the ammonium alkyl chains it is unable to cross into the organic phase (Figure 15). On basis of the benzyl bromide titration data, the TBAB cation is not sufficiently lipophilic to transport the heteronuclear aggregate to the organic phase, whereas the (n-Oct)$_4$N$^+$ cation can provide sufficient lipophilicity to carry the dimeric ion pair into the organic phase.[75]

These same interactions may also explain the inverse relationship between organic-phase phenol content and ammonium lipophilicity. Since the dimeric aggregate with (n-Bu)$_4$N$^+$ is insufficiently lipophilic for transport, phenol may displace a potassium phenoxide from the aggregate at the interphase. The newly formed homo-hydrogen-bonded complex would have less charge than the former aggregate and would now be sufficiently lipophilic for transport into the organic phase. In the case of (n-Oct)$_4$N$^+$, the dimeric aggregate readily moves into the organic phase before phenol can displace a potassium phenoxide. With the increased alkyl chain length of

(n-Oct)$_4$N$^+$, this aggregate may also be sterically inaccessible for formation of a homo-hydrogen-bonded complex.
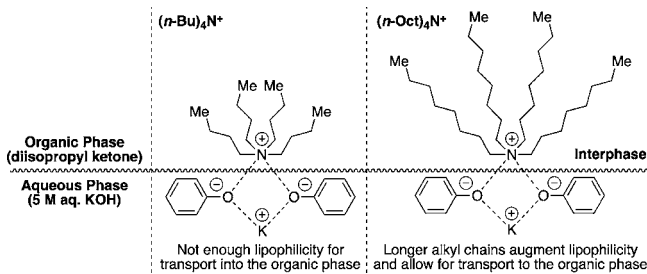

Figure 15. Proposed dimeric ion pair aggregates.

5. Tetrapropylammonium Bromide and the Third Liquid Phase. The rate of TPAB-catalyzed alkylation did not reflect the active phenoxide concentration in the organic phase. All of the spectroscopic and thermodynamic partition data suggest that this ammonium salt is hydrophilic and should lead to a slow alkylation under PTC conditions. Yet, the alkylation rate for TPAB was closer to those of the lipophilic ammonium salts than to those of the hydrophilic ammonium salts.

A reasonable explanation for the enhanced PTC alkylation rate with TPAB is the formation of a TLP. Earlier studies have conclude that the TLP in a PTC process is a catalyst-rich phase, and therefore the presence of a TLP would explain the enhanced alkylation rate for an intrinsic reaction that was first order in catalyst.[22,34,76−78] The TLP was easily observed when a full equivalent of TPAB with respect to phenol was introduced. However, no TLP was visually observed when a substoichiometric amount (0.05 or 0.10 equiv) of TPAB was employed. The inability to observe a TLP does not exclude the possibility of its existence under the reaction conditions. Sasson et al. noted the formation of a TLP in the elimination of phenethyl bromide to styrene under PTC conditions.[76] Upon closer examination, this TLP was shown to exist as a membrane around an aqueous droplet. If such a TLP were formed in reaction with a low ammonium salt content, it would be reasonable to assume that the total volume of the TLP was too low to allow coalescence of TLP droplets into a visible layer.

CONCLUSIONS

In the PTC alkylation of phenol operating by an extraction mechanism, the catalytic reactivity of linear, symmetrical tetraalkylammonium salts is directly related to their effective concentration in the organic phase, in which the alkylation reaction takes place. The range of catalytic rates spans a 663-fold difference for the series TMAB to TOAB. By comparison, the stoichiometric reactivity of the same tetraalkylammonium salts of the phenoxide homo-hydrogen-bonded dimers differs by a factor of only 6.8. Under PTC reaction conditions, the concentration of the active tetraalkylammonium phenoxide and the initial alkylation rates reach a maximum for tetrabutylammonium salts and do not increase further with more lipophilic salts. The leveling off in catalytic activity (i.e., a break in the LFER) was not the result of a change in mechanism. Titration experiments demonstrated that, for the more lipophilic salts (TBAB, THAB, TOAB), a superstoichiometric amount of phenoxide is transported to the organic phase. These experiments further revealed that a near-theoretical maximum of the ammonium phenoxide was transported to the organic phase, and the additional active phenoxide arose from the

potassium salt, which is likely shepherded into the organic phase in a higher order aggregate along with neutral phenol. The composition of these aggregates had no effect on reaction rate. Further studies on the behavior of PTC alkylation of phenol under an interfacial mechanism will be reported in due course.

ASSOCIATED CONTENT

Ⓢ Supporting Information

Detailed experimental procedures for and characterization of the ammonium phenoxides, including ^{1}H and ^{13}C NMR spectra, tables of all of the kinetic runs for alkylation of each ammonium phenoxide, stirring rate experiments, and titrations. This material is available free of charge via the Internet at http://pubs.acs.org.

AUTHOR INFORMATION

Corresponding Author
sdenmark@illinois.edu

Notes

The authors declare no competing financial interest.

ACKNOWLEDGMENTS

REFERENCES

(1) (a) Anastas, P.; Warner, J. *Green Chemistry: Theory and Practice*; Oxford University Press: Oxford, UK, 1998. (b) Weber, W. P.; Gokel, G. W. *Phase Transfer Catalysis in Organic Synthesis*; Springer-Verlag: Berlin/New York, 1977; Vol. *4*. (c) Dehmlow, E. V.; Dehmlow, S. S. *Phase Transfer Catalysis*; Verlag Chemie: Weinheim/Deerfield Beach, 1983; Vol. *11*. (d) *Phase-Transfer Catalysis: New Chemistry, Catalysts, and Applications*; American Chemical Society: Washington, DC, 1985. (e) Starks, C. M.; Liotta, C. L.; Halpern, M. *Phase-Transfer Catalysis: Fundamentals, Applications and Industrial Perspectives*; Chapman and Hall: New York, 1994. (f) *Phase-Transfer Catalysis: Mechanisms and Syntheses*; Halpern, M. E., Ed.; American Chemical Society: Washington, DC, 1997. (g) Makosza, M.; Fedorynski, M. In *Interfacial Catalysis*; Volkov, A. G., Ed.; Marcel Dekker: New York, 2003; pp 150−201.

(2) *Handbook of Phase Transfer Catalysis*; Sasson, Y., Neumann, R., Eds.; Chapman & Hall: London, 1997.

(3) Jones, R. A. *Quaternary Ammonium Salt: Their Use in Phase Transfer Catalysis*; Academic Press: London, 2001.

(4) (a) Denmark, S. E.; Gould, N. D.; Wolf, L. M. *J. Org. Chem.* **2011**, *76*, 4337−4357. (b) Denmark, S. E.; Gould, N. D.; Wolf, L. M. *J. Org. Chem.* **2011**, *76*, 4260−4336.

(5) *Ionization Constants of Organic Acids in Solution*; IUPAC Chemical Data Series No. 23, Sergent, E. P., Dempsey, B., Eds.; Pergamon Press: Oxford, 1979.

(6) Bordwell, F. G.; McCallum, R. J.; Olmstead, W. N. *J. Org. Chem.* **1984**, *49*, 1424−1427.

(7) (a) Taft, R. W.; Bordwell, F. G. *Acc. Chem. Res.* **1988**, *21*, 463−469. (b) Bordwell, F. G.; Harrelson, J. A. *Can. J. Chem.* **1990**, *68*, 1714−1718.

(8) (a) Halpern, M. *Phase Trans. Catal. Commun.* **1995**, *1*, 1−3. (b) Yang, H.-M.; Wu, H.-S. *Catal. Rev.* **2003**, *45*, 463−540.

(9) Rabinovitz, M.; Cohen, Y.; Halpern, M. *Angew. Chem., Int. Ed. Engl.* **1986**, *25*, 960−970.

(10) A companion study of the catalyst SAR for phenol alkylation under the interfacial mechanism is planned.

(11) For the most recent summary of the state of mechanistic understanding of phase transfer catalysis, see: Makosza, M.; Fedorysnki, M. *Catal. Rev.* **2003**, *45*, 321−367.

(12) Starks, C. M.; Owens, R. M. *J. Am. Chem. Soc.* **1973**, *95*, 3613−3617.

(13) Wang, M.-L. In *Handbook of Phase Transfer Catalysis*; Sasson, Y., Neumann, R., Eds.; Chapman & Hall: London, 1997; Chapter 2, pp 36−107.

(14) (a) Herriot, A. W.; Picker, D. *Tetrahedron Lett.* **1972**, *13*, 4521−4524. (b) Gordon, J. E.; Kutina, R. E. *J. Am. Chem. Soc.* **1977**, *99*, 3903−3909. (c) Herriot, A.; Picker, D. *J. Am. Chem. Soc.* **1975**, *97*, 2345−2349. (d) Landini, D.; Maia, A.; Montanari, F. *J. Am. Chem. Soc.* **1978**, *100*, 2796−2801. (e) Landini, D.; Maia, A.; Montanari, F. *J. Chem. Soc., Chem. Commun.* **1977**, 112−113.

(15) (a) Dehmlow, E. V. *Angew. Chem., Int. Ed. Engl.* **1977**, *16*, 493−505. (b) Brändström, A. *Adv. Phys. Org. Chem.* **1977**, *15*, 267−330.

(16) For an insightful analysis of hydroxide-initiated PTC reactions, see ref 1e, pp 89−108.

(17) Naik, S. D.; Doraiswamy, L. K. *Am. Inst. Chem. Eng. J.* **1998**, *44*, 612−646.

(18) (a) Wang, M.-L.; Yang, H.-M. *Chem. Eng. Sci.* **1991**, *46*, 619−627. (b) Wang, M.; Yang, H. *Ind. Eng. Chem. Res.* **1990**, *29*, 522−526.

(19) McKillop, A.; Fiaud, J.-C.; Hug, R. P. *Tetrahedron* **1974**, *30*, 1379−1382.

(20) Taft, R. W.; Bordwell, F. G. *Acc. Chem. Res.* **1988**, *21*, 463−469.

(21) (a) Wang, D. H.; Weng, H. S. *J. Chin. Inst. Chem. Eng.* **1996**, *27*, 129−139. (b) Weng, H. S.; Wang, D. H. *J. Chin. Inst. Chem. Eng.* **1996**, *27*, 419−426. (c) Wang, D. H.; Weng, H. S. *J. Chin. Inst. Chem. Eng.* **1995**, *26*, 147−156. (d) Wang, D. H.; Weng, H. S. *J. Eng. Sci.* **1995**, *50*, 3477.

(22) Yadav, G. D.; Desai, N. M. *Org. Process Res. Dev.* **2005**, *9*, 749−756.

(23) (a) Makosza, M. *Tetrahedron Lett.* **1966**, *7*, 4261−4624. (b) Makosza, M. *Pure Appl. Chem.* **1975**, *43*, 439−462. (c) Makosza, M.; Bialecka, E. *Tetrahedron Lett.* **1977**, *18*, 183−186.

(24) (a) Halpern, M.; Sasson, Y.; Willner, I.; Rabinovitz, M. *Tetrahedron Lett.* **1981**, *22*, 1719−1722. (b) Halpern, M.; Sasson, Y.; Rabinovitz, M. *J. Org. Chem.* **1983**, *48*, 1022−1025. (c) Halpern, M.; Sasson, Y.; Rabinovitz, M. *J. Org. Chem.* **1984**, *49*, 2011−2012. (d) Halpern, M.; Feldman, D.; Sasson, Y.; Rabinovitz, M. *Angew. Chem.* **1984**, *96*, 79−80. (e) Halpern, M.; Zahalaka, H. A.; Sasson, Y.; Rabinovitz, M. *J. Org. Chem.* **1985**, *50*, 5088−5092. (f) Feldman, D.; Halpern, M.; Rabinovitz, M. *J. Org. Chem.* **1985**, *50*, 1746−1749.

(25) *Synthetic and Natural Phenols*; Tyman, J. H. P., Ed.; Elsevier: Amsterdam, 1996; Vol. *52*.

(26) Lewis, E. S.; Vanderpool, S. *J. Am. Chem. Soc.* **1977**, *99*, 1946−1949.

(27) For an overview and discussion of theoretical derivations of ammonium ion pair reactivity, see : *Ions and Ion Pairs in Organic Reactions*; Szwarc, M., Ed.; John Wiley & Sons: New York, 1974; Vols. *1* and *2*.

(28) Ugelstad, J.; Ellingsen, T.; Berge, A. *Acta Chim. Scand* **1966**, *20*, 1593−1598.

(29) Starks, C. M. In *Phase-Transfer Catalysis*; Halpern, M. E., Ed.; American Chemical Society: Washington, DC, 1997; Vol. *659*, Chapter 2, pp 2−10.

(30) Reference 1e, p 86.

(31) (a) Brändström, A.; Junggren, U. *Acta Chem. Scand.* **1969**, *23*, 2203−2204. (b) Brändström, A; Junggren, U. *Acta Chem. Scand.* **1969**, *23*, 2204−2205. (c) Brändström, A.; Junggren, U. *Acta Chem. Scand.* **1969**, *23*, 2536−2537. (d) Brändström, A.; Junggren, U. *Acta Chem. Scand.* **1969**, *23*, 3585−3586. (e) Brändström, A. *Pure Appl. Chem.* **1982**, *54*, 1769−1782.

(32) Wilson, K.; Adams, D. J.; Rothenberg, G.; Clark, J. H. *J. Mol. Catal. A: Chem.* **2000**, *159*, 309−314.

(33) Wang, M.-L. In *Handbook of Phase Transfer Catalysis*; Sasson, Y., Neumann, R., Eds.; Chapman & Hall: London, 1997; Chapter 2, pp 36−107.

(34) Wang, D.-H.; Weng, H.-S. *Chem. Eng. Sci.* **1988**, *43*, 2019−2024.

(35) Mason, D.; Magdassi, S.; Sasson, Y. *J. Org. Chem.* **1991**, *56*, 7229−7232.

(36) Bordwell, F. G.; Hughes, D. L. *J. Org. Chem.* **1982**, *47*, 3224−3232.

(37) Caulton, K. G.; Chisholm, M. H.; Drake, S. R.; Folting, K.; Huffman, J. C.; Streib, W. E. *Inorg. Chem.* **1993**, *32*, 1970−1976.

(38) (a) Dinnebier, R. E.; Pink, M.; Sieler, J.; Norby, P.; Stephens, P. W. *Inorg. Chem.* **1998**, *37*, 4996−5000. (b) Dinnebier, R. E.; Pink, M.; Sieler, J.; Stephens, P. W. *Inorg. Chem.* **1997**, *36*, 3398−3401.

(39) Fraser, M. E.; Fortier, S.; Markiewicz, M. K.; Rodrigue, A.; Bovenkamp, J. W. *Can. J. Chem.* **1987**, *65*, 2558−2563.

(40) Caulton, K. G.; Chisholm, M. H.; Drake, S. R.; Folting, K.; Huffman, J. C.; Streib, W. E. *Inorg. Chem.* **1993**, *32*, 1970−1976.

(41) See, for example: (a) Chantooni, M. K., Jr.; Kolthoff, I. M. *J. Phys. Chem.* **1976**, *80*, 1306−1310. (b) Arnett, E. M.; Moriarity, T. C.; Small, L. E.; Rudolph, J. P.; Quirk, R. P. *J. Am. Chem. Soc.* **1973**, *95*, 1492−1495. (c) Arnett, E. M.; Small, L. E.; Oancea, D.; Johnston, D. *J. Am. Chem. Soc.* **1976**, *98*, 7346−7350. (d) Arnett, E. M.; Venkatasubramanium, K. G. *J. Org. Chem.* **1983**, *48*, 1569−1578. (e) Silva, P. J. *J. Org. Chem.* **2009**, *74*, 914−916.

(42) Nielsen, M. F.; Hammerich, O. *Acta Chem. Scand.* **1989**, *43*, 269−274.

(43) Goddard, R.; Reetz, M.; Herzog, M. *Tetrahedron* **2002**, *58*, 7847−7850.

(44) Based on a search of the Cambridge Structural Database on April 27, 2011, in combination with energy minimization of monomeric sodium and potassium phenolates (6-31G*//RHF).

(45) Viout, P. *J. Mol. Catal.* **1981**, *10*, 231−240.

(46) Minot, C.; Trong, N. A. *Tetrahedron Lett.* **1975**, *16*, 3905−3908.

(47) (a) Johnson, M. L.; Rodriguez, C.; Benjamin, I. *J. Phys. Chem. A* **2009**, *113*, 2086−2091. (b) Nelson, K. V.; Benjamin, I. *Chem. Phys. Lett.* **2011**, *508*, 59−62.

(48) (a) Nelson, K. V.; Benjamin, I. *J. Phys. Chem. C* **2010**, *114*, 1154−1163. (b) Nelson, K. V.; Benjamin, I. *J. Phys. Chem. C* **2011**, *115*, 2290−2296.

(49) Pradines, V.; Poteau, R.; Pimienta, V. *Eur. J. Chem Phys. Phys. Chem* **2007**, *8*, 1524−1533.

(50) Coleman, M. T.; Leblanc, G. *Org. Process Res. Dev.* **2010**, *14*, 732−736.

(51) Harlow, G. A.; Noble, C. M.; Wyld, G. E. A. *Anal. Chem.* **1956**, *28*, 787−791.

(52) Abrams, I. M.; Millar, J. R. *React. Funct. Polym.* **1997**, *35*, 7−22.

(53) For tables of the titration data, see Supporting Information.

(54) Section 6: Fluid Properties. *CRC Handbook of Chemistry and Physics*, 92nd ed.; Haynes, W. M., Lide, D. R., Eds.; CRC Press: Boca Raton, FL, 2011−2012; pp 212 − 228.

(55) Hopkins, R. N.; Yerger, E. S.; Lynch, C. C. *J. Am. Chem. Soc.* **1939**, *61*, 2460−2461.

(56) Schneider, C. H.; Lynch, C. C. *J. Am. Chem. Soc.* **1943**, *65*, 1063−1066.

(57) The solubility of DIPK in H_2O at 20 °C is 45.5 mM: Section 5: Aqueous Solubility and Henry's Law Constants of Organic Compounds. *CRC Handbook of Chemistry and Physics*, 92nd ed.; Haynes, W. M., Lide, D. R., Eds.; CRC Press: Boca Raton, FL, 2011−2012.

(58) For sodium and potassium homo-hydrogen-bonded phenoxide complex synthesis, see the Supporting Information.

(59) For the the raw data and kinetic plots, see the Supporting Information.

(60) The background alkylation rate was found to be 2.99×10^{-8} mol L^{-1} s^{-1}.

(61) For a recent instructive analysis of nonlinear membrane permeability−lipophilicity models, see: Balaz, S. *Chem. Rev.* **2009**, *109*, 1793−1899.

(62) Anslyn, E. V.; Dougherty, D. *Modern Physical Organic Chemistry*; University Science Books: Sausalito, CA, 2006; Chapters 7−9.

(63) For experimental details (calibration, raw data, etc.), see the Supporting Information.

(64) Studies in medicinal chemistry have shown repeatedly that the contribution of a methylene unit to $ClogP_{(o/w)}$ is additive for homologous series like quaternary ammonium ions. See: (a) Hansch, C. *Acc. Chem. Res.* **1969**, *2*, 232−239. (b) Hansch, C.; Kurup, A.; Garg, R.; Gao, H. *Chem. Rev.* **2001**, *101*, 619−672.

(65) The effective phenoxide concentration of the TLP was calculated at 1620 mM; the starting aqueous phase concentration was 759 mM.

(66) Sawada, K.; Chigira, F. *J. Mol. Liq.* **1995**, *65/66*, 265−268.

(67) Price, F. P., Jr.; Hammett, L. P. *J. Am. Chem. Soc.* **1941**, *63*, 2387−2393.

(68) Reference 1c, p 13.

(69) (a) Gustavii, K.; Schill, G. *Acta Pharm. Suec* **1966**, *3*, 241−258. (b) Gustavii, K.; Schill, G. *Acta Pharm. Suec* **1966**, *3*, 259−268. (c) Gustavii, K. *Acta Pharm. Suec* **1967**, *4*, 233−246.

(70) For this comparison, the rate constants are normalized to the rate for the uncatalyzed reaction (i.e., $K^+OPh]^-$.)

(71) For recent reviews of the application of QSAR methodology to catalytic acitivty, see: (a) Burello, E.; Rothenberg, G. *Int. J. Mol. Sci* **2006**, *7*, 375−404. (b) Maldonado, A. G.; Rothenberg, G. *Chem. Soc. Rev.* **2010**, *39*, 1891−1902.

(72) Buchwald, P. *J. Pharm. Sci.* **2005**, *94*, 2355−2379.

(73) This assertion is supported by the demonstration that the concentration of the reactive species Q^+PhO^- continues to increase in partitioning experiments with 0.6 equiv of tetraalkylammonium salts: $(n\text{-}Bu)_4N^+$, 47.1% transport, and $(n\text{-}Oct)_4N^+$, 63.2% transport.

(74) (a) Dehmlow, E. V.; Thieser, R.; Sasson, Y.; Pross, E. *Tetrahedron* **1985**, *41*, 2927−2932. (b) Zerda, J.; Sasson, Y. *J. Chem. Soc., Perkin Trans. 2* **1987**, 1147−1151.

(75) Such supramolecular structures have been identified for transport of hydrogen peroxide in ruthenium-catalyzed oxidations. Sasson et al. have identified the formation of vesicles as the mechanism of transport of hydrogen peroxide: Rothenberg, G.; Barak, G.; Sasson, Y. *Tetrahedron* **1999**, *55*, 6301−6310.

(76) Mason, D.; Magdassi, S.; Sasson, Y. *J. Org. Chem.* **1991**, *56*, 7229−7232.

(77) Wang, D.-H.; Weng, H.-S. *Chem. Eng. Sci.* **1995**, *50*, 3477−3486.

(78) Mąkosza, M.; Kryłowa, I. *Tetrahedron* **1999**, *55*, 6395−6402.